

# Measuring easily electron plasma densities in gases produced by ultrashort lasers and filaments

D. Abdollahpour,<sup>1,2,\*</sup> S. Suntsov,<sup>1</sup> D. G. Papazoglou,<sup>1,3</sup> and S. Tzortzakis<sup>1,3</sup>

<sup>1</sup>*Institute of Electronic Structures and Laser, Foundation for Research and Technology Hellas, P.O. Box 1527, 71110, Heraklion, Greece*

<sup>2</sup>*Physics Department, University of Crete, 71003, Heraklion, Greece*

<sup>3</sup>*Materials Science and Technology Department, University of Crete, 71003, Heraklion, Greece*

\*[dabdolah@iesl.forth.gr](mailto:dabdolah@iesl.forth.gr)  
<http://umis.iesl.forth.gr>

**Abstract:** We present an easy way to calibrate the simple plasma conductivity (PCo) technique for measuring electron plasma densities in gases. We show that calibration can be achieved using a single absolute plasma density measurement through an independent analytical technique, in our case the in-line holographic microscopy (i-HOM). We show the validity and power of the method by comparing the calibrated PCo with results from i-HOM over an extended range of experimental parameters.

© 2011 Optical Society of America

**OCIS codes:** (320.7110) Ultrafast nonlinear optics; (350.5400) Plasmas; (280.5395) Plasma diagnostics.

---

## References and links

1. A. Couairon and A. Mysyrowicz, "Femtosecond filamentation in transparent media," *Phys. Rep.* **441**(2-4), 47–189 (2007).
2. S. Tzortzakis, B. Prade, M. Franco, A. Mysyrowicz, S. Hüller, and P. Mora, "Femtosecond laser-guided electric discharge in air," *Phys. Rev. E Stat. Nonlin. Soft Matter Phys.* **64**(5), 057401 (2001).
3. G. Méjean, J. Kasparian, E. Salmon, J. Yu, J. P. Wolf, R. Bourayou, R. Sauerbrey, M. Rodriguez, L. Wöste, H. Lehmann, B. Stecklum, U. Laux, J. Eislöffel, A. Scholz, and A. P. Hatzes, "Towards a supercontinuum-based infrared lidar," *Appl. Phys. B* **77**, 357–359 (2003).
4. S. Tzortzakis, D. Anglos, and D. Gray, "Ultraviolet laser filaments for remote laser-induced breakdown spectroscopy (LIBS) analysis: applications in cultural heritage monitoring," *Opt. Lett.* **31**(8), 1139–1141 (2006).
5. S. Eisenmann, A. Pukhov, and A. Zigler, "Fine structure of a laser-plasma filament in air," *Phys. Rev. Lett.* **98**(15), 155002 (2007).
6. S. Tzortzakis, M. A. Franco, Y. B. André, A. Chiron, B. Lamouroux, B. S. Prade, and A. Mysyrowicz, "Formation of a conducting channel in air by self-guided femtosecond laser pulses," *Phys. Rev. E Stat. Phys. Plasmas Fluids Relat. Interdiscip. Topics* **60**(4), R3505–R3507 (1999).
7. S. Akturk, B. Zhou, M. Franco, A. Couairon, and A. Mysyrowicz, "Generation of long plasma channels in air by focusing ultrashort laser pulses with an axicon," *Opt. Commun.* **282**, 129–134 (2009).
8. D. Abdollahpour, P. Panagiotopoulos, M. Turconi, O. Jedrkiewicz, D. Faccio, P. Di Trapani, A. Couairon, D. G. Papazoglou, and S. Tzortzakis, "Long spatio-temporally stationary filaments in air using short pulse UV laser Bessel beams," *Opt. Express* **17**(7), 5052–5057 (2009).
9. S. Rebibo, J. P. Geindre, P. Audebert, G. Grillon, J. P. Chambaret, and J. C. Gauthier, "Single-shot spectral interferometry of femtosecond laser-produced plasmas," *Laser Part. Beams* **19**(1), 67–73 (2001).
10. C. Y. Chien, B. La Fontaine, A. Desparois, Z. Jiang, T. W. Johnston, J. C. Kieffer, H. Pépin, F. Vidal, and H. P. Mercure, "Single-shot chirped-pulse spectral interferometry used to measure the femtosecond ionization dynamics of air," *Opt. Lett.* **25**(8), 578–580 (2000).
11. J. P. Geindre, P. Audebert, A. Rousse, F. Fallières, J. C. Gauthier, A. Mysyrowicz, A. D. Santos, G. Hamoniaux, and A. Antonetti, "Frequency-domain interferometer for measuring the phase and amplitude of a femtosecond pulse probing a laser-produced plasma," *Opt. Lett.* **19**(23), 1997–1999 (1994).
12. S. Minardi, A. Gopal, M. Tatarakis, A. Couairon, G. Tamosauskas, R. Piskarskas, A. Dubietis, and P. Di Trapani, "Time-resolved refractive index and absorption mapping of light-plasma filaments in water," *Opt. Lett.* **33**(1), 86–88 (2008).
13. S. Tzortzakis, B. Prade, M. Franco, and A. Mysyrowicz, "Time-evolution of the plasma channel at the trail of a self-guided IR femtosecond laser pulse in air," *Opt. Commun.* **181**(1-3), 123–127 (2000).
14. Z. Liu, M. Centurion, G. Panotopoulos, J. Hong, and D. Psaltis, "Holographic recording of fast events on a CCD camera," *Opt. Lett.* **27**(1), 22–24 (2002).

15. M. Centurion, Y. Pu, Z. Liu, D. Psaltis, and T. W. Hänsch, "Holographic recording of laser-induced plasma," *Opt. Lett.* **29**(7), 772–774 (2004).
  16. D. G. Papazoglou and S. Tzortzakis, "In-line holography for the characterization of ultrafast laser filamentation in transparent media," *Appl. Phys. Lett.* **93**(4), 041120–041123 (2008).
  17. G. Rodríguez, A. R. Valenzuela, B. Yellampalle, M. J. Schmitt, and K.-Y. Kim, "In-line holographic imaging and electron density extraction of ultrafast ionized air filaments," *J. Opt. Soc. Am. B* **25**(12), 1988–1997 (2008).
  18. S. A. Hosseini, B. Ferland, and S. L. Chin, "Measurement of filament length generated by an intense femtosecond laser pulse using electromagnetic radiation detection," *Appl. Phys. B* **76**, 583–586 (2003).
  19. A. Becker, N. Aközbeke, K. Vijayalakshmi, E. Oral, C. M. Bowden, and S. L. Chin, "Intensity clamping and re-focusing of intense femtosecond laser pulses in nitrogen molecular gas," *Appl. Phys. B* **73**, 287–290 (2001).
- 

## 1. Introduction

Filamentation of ultrashort laser pulses, as one of the main features of nonlinear optical pulse propagation effects, has attracted lots of interest in the last years. For laser beams whose pulse power exceeds the critical power of self-focusing, the beam undergoes self-focusing and, as the intensity of the beam becomes higher and higher, ionization of the medium can occur through tunnel ionization, multiphoton ionization, and avalanche, depending on the pulse duration and the medium. A dynamic competition between self-focusing and plasma defocusing (together with additional linear and nonlinear effects) leads to the filamentary propagation of the laser beam [1]. A filament has an almost constant narrow waist over propagation lengths much longer than the corresponding Rayleigh range. The capability of transferring high powers and creating long continuous plasma channels through filamentation has found many applications in different fields such as lightning control [2], LIDAR [3], remote LIBS [4], etc. Thus, characterizing the laser generated plasma strings in a quantitative manner is of crucial importance for both the fundamental understanding of the nonlinear optical pulse propagation and applications.

A number of approaches have been used for the characterization of the low-density filament generated plasmas. Among the most widely used approaches are the plasma electrical conductivity [5–8], interferometric techniques [9–11], holographic methods [12–17], backward emitted nitrogen fluorescence and acoustic wave generation from plasma [18]. All these approaches can be grouped in two categories. The first one includes analytical methods such as holography and interferometry that are capable of spatiotemporally resolving the plasma density distribution. These methods, although accurate, are quite complex in their implementation and cannot be practically used to measure the plasma distribution over an extended filamentation length, which may reach many meters. Moreover, they usually have a resolving limit that does not allow the study of low-density plasma strings. The second category involves spatiotemporally averaging methods such as plasma conductivity and plasma emission that are much simpler and straightforward in their implementation but difficult and tricky to calibrate. A simple and at the same time quantitative technique for measuring electron densities would prove most useful for the large scientific community working in this field.

In this paper, we show that the plasma conductivity technique (PCo) can be calibrated based on a simple physical model. The validity of our approach is confirmed by comparing the calibrated electrical conductivity measurements with the results of in-line holographic microscopy (i-HOM) [16], which provides us with accurate measurements of the plasma electron densities.

## 2. Experimental setup and physical model

The output of an amplified Ti:Sapphire laser delivering 35 fs laser pulses at a central wavelength of 800 nm with pulse energies up to 30 mJ operating at 50 Hz repetition rate (beam waist of 12.5 mm) was used to create plasma filaments in different focusing geometries. The schematic of the experimental setup is shown in Fig. 1(a). The laser generated plasma strings were positioned in the area in-between two identical, 1 mm in diameter, metallic cylindrical rods (electrodes) separated by 3 mm. The electrodes were connected to a DC high voltage (1.4 kV) source. Undesired direct illumination of the electrodes by the laser beam was blocked using a Teflon aperture placed in front of them. The

emergence of laser generated plasma between the electrodes in the presence of the external DC electric field leads to a transient current flow in the circuit.

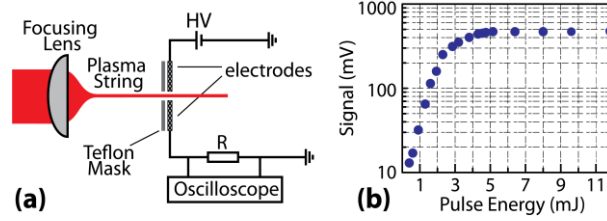


Fig. 1. (a) PCo experimental setup scheme, and (b) peak PCo signal vs. laser pulse energy for a plasma channel created by focusing the laser beam using an  $f=100$  mm lens.

This transient current is measured as a voltage drop across a resistance ( $R = 8$  k $\Omega$ ) using a probe connected to an oscilloscope (see Fig. 1(a)). The applied high voltage was chosen in such a way to ensure the linear operation of the circuit, i.e. linear increase of the signal with increased applied voltage. The impedance and capacitance of the oscilloscope were 1 M $\Omega$  and 16 pF, respectively. It can be easily found that the response time of such a circuit is in the order of 0.1  $\mu$ s, much longer than the sub-nanosecond lifetime of femtosecond laser generated plasmas in air [13].

A simple physical model will help us understand the mechanism that leads to the transient perturbation and to derive a quantitative relation between the plasma density and the measured current. It is well known that under the action of a strong electrostatic field a charge separation is created between electrons and ions in the plasma. For each electron-ion pair the induced dipole moment is  $\mathbf{p} = q \cdot dz$  where  $q$  is the electron charge and  $dz$  is the electron-ion separation. Thus, the total induced polarization  $\mathbf{P}$  in the plasma volume is  $\mathbf{P} = \langle n_e \rangle \mathbf{p} = \langle n_e \rangle q \cdot dz$ , where  $\langle n_e \rangle$  is the spatially averaged plasma density. This induced polarization will generate an electric field that will affect the total electric field between the electrodes and under a rather general approach can be approximated as:

$$\mathbf{E}' \propto \mathbf{P} \cdot V_p \Rightarrow \mathbf{E}' \propto \langle n_e \rangle r_p^2 l_p \quad (1)$$

where  $V_p$  is the plasma volume,  $r_p$  is the plasma radius and  $l_p$  is the plasma length. The electric field generated by this dipole perturbs the total electric field and consequently leads to a voltage drop between the electrodes. Charge trapping in the plasma through recombination eventually stops the process. In response to this perturbation and in order to keep the voltage constant, the HV generator provides extra charges to the electrodes that counter balance the perturbation. This charge flow towards the electrodes creates a transient current  $I_R$  that is probed as the voltage drop across the resistance  $R$ . Taking into account the response time of the high voltage circuit, this transient current is proportional to the temporal convolution of the plasma induced transient perturbation and the impulse response of the measuring circuit. Numerical simulations, using the plasma decay rates in air and the slow response time of such electrical circuits, show [7] that in the electron density regime up to  $10^{17}$  cm $^{-3}$  there is a linear correlation between the peak electron density and the peak current. Though, since the perturbation is related to the induced polarization under the applied HV, its temporal evolution process is even more complex and as we will see in the following our experimental measurements confirm that the proportionality holds, within the experimental error, for even higher electron densities. Under this perspective the transient current flow through the resistance, and consequently the measured voltage change  $\Delta V$  is proportional to the initial perturbation:

$$\Delta V = I_R \cdot R \propto \langle n_e \rangle r_p^2 l_p R \quad (2)$$

The proportionality in Eq. (2) inhibits the direct estimation of the average electron density of a laser generated plasma string by a single measurement. On the other hand, this technique can be calibrated to provide absolute electron density values if one could use a reference measurement, where both electron density and plasma dimensions are known. Let us assume that a reference voltage change (signal) due to the presence of a plasma string with known dimensions and known electron density is  $\Delta V^{ref} \propto \langle n_e^{ref} \rangle (r_p^{ref})^2 l_p^{ref}$ . Likewise, the signal from a different plasma string with known dimensions but unknown electron density can be written as  $\Delta V \propto \langle n_e \rangle r_p^2 l_p$ . Therefore, from the ratio of the two measured signals  $\Delta V / \Delta V^{ref}$ , the unknown electron density  $\langle n_e \rangle$  can be estimated as:

$$\langle n_e \rangle = \left( r_p^{ref} / r_p \right)^2 \left( l_p^{ref} / l_p \right) \left( \Delta V / \Delta V^{ref} \right) \langle n_e^{ref} \rangle \quad (3)$$

This formula shows that the average electron density of an arbitrary plasma string can be measured if the electron density of a reference plasma string is known. Furthermore, the spatial dimensions of the plasma and more particular their ratio to the dimensions of the reference plasma should be used as a geometric correction factor to the measured signal ratio. Using this technique the plasma distribution for plasma string lengths shorter than the diameter of the electrodes ( $< 1$  mm in our case) cannot be revealed. On the other hand, in extended plasma strings such as those created through filamentation, the longitudinal distribution of the electron density can be measured by translating the electrodes along the propagation direction. The longitudinal spatial resolution is then determined by the diameter of the electrodes. The temporal evolution of the plasma density is practically lost in such a measurement since the measured signal is proportional to the peak value of the plasma density in time.

### 3. Results and discussion

Experimentally, plasma filaments were created using the 35 fs laser beam at different input pulse energies and focusing it in air using plano-convex lenses of various focal lengths. In all cases, the electrodes were placed equidistantly from the plasma string at a longitudinal position where the signal was maximized. A typical measured peak signal versus laser pulse energy for the case of a lens with focal length of  $f = 100$  mm (F-Number: #F=4) is shown in Fig. 1(b). The signal increases rapidly as a function of the input energy for energies up to  $\sim 2$  mJ. This strong, nearly exponential, increase is the result of the increase of the plasma string average electron density and its thickness (see Eq. (2)). At higher input energies saturation is observed due to intensity clamping in the filament [19].

As already mentioned above, the average electron density of an arbitrary plasma string can be measured from such a signal if the electron density of a reference plasma along with the spatial dimensions of both plasma strings are known. Also, the reference plasma string should be generated using similar laser pulse durations as we will discuss in the following. A very simple method to measure the plasma dimensions is to image its fluorescence emission.

Plasma string fluorescence images were recorded on a transverse plane using a linear CCD camera. Since we are interested in the relative string dimensions a conventional photographic camera could also be used for this purpose. Figure 2(a) presents the fluorescence images of the plasma strings corresponding to the measurements shown in Fig. 1(b). As can be seen from the images, the size of the plasma string strongly depends on the laser pulse energy.

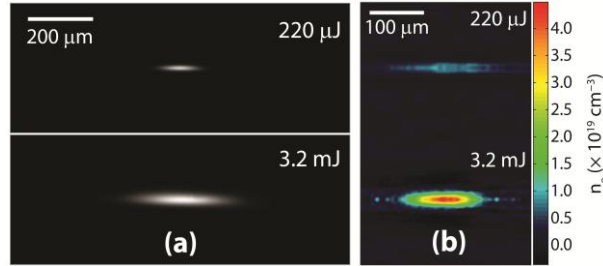


Fig. 2. (a) Transverse CCD images of plasma fluorescence for different laser pulse energies, and (b) corresponding retrieved spatial distribution of the electron density using i-HOM.

Now, having a simple method for measuring the plasma string dimensions, we only need a reference measurement of electron density. For this purpose, we used the i-HOM technique which is capable of retrieving the 3D distribution of the electron density of micrometer sized laser generated plasma strings with a temporal resolution of  $< 50$  fs and is described in detail in [16]. Briefly, this pump-probe method is capable of retrieving very small phase/amplitude changes of the probe beam wavefront as a result of a pump-induced modification of the medium. The pump in our case is the filament plasma string. A transversally propagating collimated probe beam passes through the plasma and consequently its phase and/or amplitude is modified due to the presence of the plasma string. In-line holograms of the propagating perturbed probe beam are recorded on a CCD camera at different positions along the probe propagation direction. The recorded intensity patterns (in-line holograms) are then fed into an iterative wavefront propagation algorithm which accurately retrieves the amplitude and phase of the perturbed wavefront. Finally, the 3D distribution of the real and the imaginary parts of the refractive index perturbation are obtained using Abel inversion. The electron density  $n_e$  in the plasma string is estimated using a simple Drude model  $n_e = -2n_{cr} \cdot \Delta n$ , where  $n_{cr} = 1.7 \times 10^{21} \text{ cm}^{-3}$  is the critical plasma density in air for the 800 nm probe pulse. Figure 2(b) shows the i-HOM retrieved spatial distribution of the electron density for the two cases of Fig. 2(a) just after the passage of the pump pulse (maximum electron density).

In Fig. 3(a) are shown the results from the i-HOM together with the corresponding calibrated PCo measurements for filaments created with a 100 mm ( $\#F=4$ ) focusing lens at different energies. As a reference for the calibration, we have chosen the i-HOM measurement at 3.2 mJ averaged over 1 mm along the propagation direction, since this is the minimal longitudinal spatial resolution of our PCo technique, defined by the diameter of the electrodes.

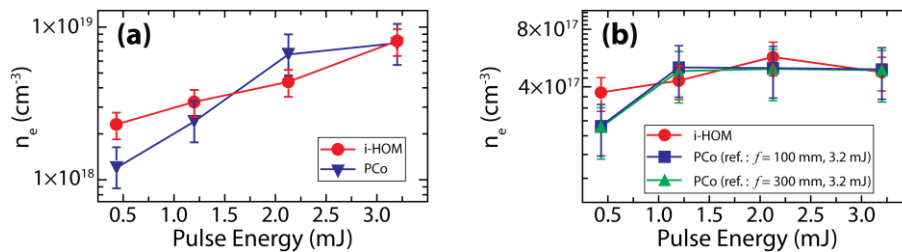


Fig. 3. i-HOM- and calibrated PCo-measured electron densities vs. input pulse energy for plasma strings created by  $f = 100$  mm (a), and  $f=300$  mm (b) lenses (see text for calibration details).

In order to confirm that the calibration method does not depend on the focusing geometry we have repeated the same experiments with a 300 mm focusing lens ( $\#F=12$ ). In Fig. 3(b) are shown the results from the i-HOM together with the calibrated PCo measurements using two different reference measurements, one using the 100 mm lens and the other using the 300 mm

lens (both at 3.2 mJ). The results are clear and indicate that our method is not sensitive to the reference choice or the focusing geometry. Thus, from the above, it's clear that the calibrated PCo technique is capable of providing an adequate estimation of the average electron density of a plasma string. Furthermore, beyond the much simpler implementation, the calibrated PCo technique can be used to study plasma strings with electron densities below the sensitivity threshold of i-HOM (plasma densities above  $10^{17} \text{ cm}^{-3}$  are needed).

Finally, we verified that our calibration is also valid for different laser pulse durations. As mentioned earlier, it is well known that the contribution of different ionization mechanisms in plasma formation depends on the pulse duration. For longer pulse durations, contribution of the avalanche ionization becomes more significant than the tunnel ionization and the multiphoton ionization and therefore the generated plasma densities in this regime are expected to be higher. Another set of experiments was performed in order to study the effect of the laser pulse duration on the plasma density. For our calibration, a plasma string generated by focusing 3.2 mJ, 35 fs, 800 nm pulses using an  $f=100$  mm lens ( $\#F=4$ ) was used as a reference. The pulse duration was then changed by adding chirp on the pulses, through adjustment of the distance between the two gratings in the compressor of our laser system. The pulse duration was measured using a single shot autocorrelator. The measured electron densities as a function of the pulse energy for pulse durations ranging from 35 to 200 fs are shown in Fig. 4. As expected; the generated plasma electron densities are higher for longer pulse durations due to the increased avalanche contribution. We note that the technique can be used for even longer pulses but one should perform a specific calibration using a reference with similar pulse duration.

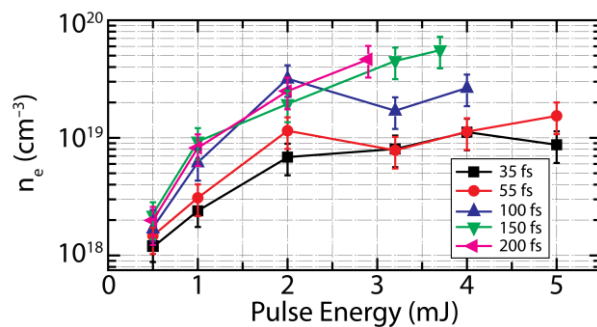


Fig. 4. Estimated electron density from calibrated PCo measurements in plasma strings using different laser pulse durations and energies ( $f=100$  mm).

#### 4. Conclusion

In summary, we have proposed an effective way to calibrate the plasma conductivity technique for measuring plasma electron densities in gases. We have demonstrated that the calibration can be achieved using a single reference measurement from another analytical technique such as in-line holography. This enables a simple, fast, and fairly accurate measurement of the electron density of laser-generated plasmas in gaseous media and more specifically of extended plasma strings that are generated during the filamentation of ultrashort laser pulses. The calibrated PCo technique is expected to be a very useful tool for researchers working with strong fields and nonlinear propagation phenomena.

#### Acknowledgments

This work was supported by the European Union (EU) Marie Curie Excellence Grant "MULTIRAD" MEXT-CT-2006-042683. This work was also partially supported by the EU FP7 project, PHOME (FET Contract No. 213390).